Journal Pre-proof

Aqueous two-phase system formed by polyethylene glycol methyl ether 550 and choline-based ionic liquids: from phase diagrams to application in the extraction of proteins

Tairan Eutimio dos Santos, Milena Santos Leite, Ranyere Lucena de Souza, Matheus Mendonça Pereira, Mara G. Freire, Cleide Mara Faria Soares, A.Álvaro Silva Lima

PII: S1369-703X(26)00156-7

DOI: https://doi.org/10.1016/j.bej.2026.110225

Reference: BEJ110225

To appear in: *Biochemical Engineering Journal*

Please cite this article as: Tairan Eutimio dos Santos, Milena Santos Leite, Ranyere Lucena de Souza, Matheus Mendonça Pereira, Mara G. Freire, Cleide Mara Faria Soares and A.Álvaro Silva Lima, Aqueous two-phase system formed by polyethylene glycol methyl ether 550 and choline-based ionic liquids: from phase diagrams to application in the extraction of proteins, *Biochemical Engineering Journal,* (2026) doi:https://doi.org/10.1016/j.bej.2026.110225

Aqueous two-phase system formed by polyethylene glycol methyl ether 550 and choline-based ionic liquids: from phase diagrams to application in the extraction of proteins

Tairan Eutimio dos Santos[1], Milena Santos Leite[1], Ranyere Lucena de Souza[1,2], Matheus Mendonça Pereira[3], Mara G. Freire[4], Cleide Mara Faria Soares[1,2], Álvaro Silva Lima[5]

[1] University Tiradentes. Av. Murilo Dantas, 300. Farolândia. 49032-490. Aracaju-Sergipe.

[2] Instituto de Tecnologia e Pesquisa. Av. Murilo Dantas, 300, Prédio do ITP. Farolândia. 49032-490. Aracaju-Sergipe.

[3] University of Coimbra, CERES, Department of Chemical Engineering, Rua Sílvio Lima, Pólo II – Pinhal de Marrocos, 3030-790 Coimbra, Portugal

[4] CICECO - Aveiro Institute of Materials, Department of Chemistry, University of Aveiro, 3810-193 Aveiro, Portugal

[5] Federal University of Bahia. Graduated Programm on Chemical Engeneering. Rua Aristides Novis, 2. Federação, 40210-630, Salvador-BA, Brazil.

Corresponding author: E-mail: aslima2001@yahoo.com.br

Abstract

Aqueous two-phase systems (ATPSs) are promising liquid–liquid platforms for protein extraction and purification. In this study, novel ATPSs composed of choline-based ionic liquids (ILs) and polyethylene glycol methyl ether (PEGME 550) were characterized and then evaluated for protein separation. Phase diagrams were determined by turbidimetry at 298 K and 0.1 MPa, indicating that phase formation is governed by hydrogen-bonding interactions between IL ions and water, promoting the salting-out effect. The largest biphasic region was observed for choline bitartrate ([Ch][BIT]) systems. Separation performance was assessed using bovine serum albumin – BSA (model protein), and immunoglobulin G – IgG (biopharmaceutical compound). BSA partitioning was studied in systems containing 45 wt% PEGME 550 and 40 wt% IL, while IgG extraction was evaluated under different compositions and temperatures. BSA preferentially migrated to the IL-rich (bottom) phase, mainly driven by electrostatic interactions and hydrogen bonding, reaching extraction efficiencies up to 55% ([Ch][BIT] and choline dihydrogen citrate ([Ch][DHC]). Protein stability analysis via amide I spectral deconvolution showed minor structural changes, especially in [Ch]Cl systems. Consequently, [Ch]Cl-based ATPSs were selected for IgG extraction, where increasing temperature from 298 to 318 K improved efficiency to 49%, while preserving structural integrity. Molecular docking supported the experimental findings by elucidating IL–protein interactions, highlighting the potential of [Ch]Cl-based ATPSs as effective platforms for IgG purification.

Keywords: Aqueous two-phase system, partitioning, immunoglobulin G, protein stability.

1. Introduction

The demand for low-cost, simple, and sustainable processes for extracting and purifying high-value proteins is increasing. In this context, aqueous two-phase systems (ATPSs) have been widely explored due to their sustainability, mild conditions, and high biocompatibility [1–3]. ATPSs are formed by two water-soluble compounds that, above critical concentrations, separate into immiscible aqueous phases with high capacity for biomolecule extraction and purification [4,5]. They are widely used for processing proteins, enzymes, pigments, antibodies, and antioxidants, highlighting their efficiency

and relevance in biotechnological applications [6–10]. These systems are described by phase diagrams showing compositions at thermodynamic equilibrium. Selecting mixture points in the biphasic region and their tie lines enables their use as separation and enrichment platforms, since phases share properties like density and viscosity but differ in mass and volume [11].

In general, phase-forming components of ATPSs include polymers, inorganic and organic salts, sugars, ionic liquids, organic solvents, and deep eutectic solvents. Among the various possible combinations, polymer/salt and polymer/ionic liquid systems are the most reported [12,13]. The formation of polymer-based ATPSs is closely related to the intrinsic hydrophobicity of the polymers. Polyethylene glycol (PEG), a widely used synthetic polymer, exhibits unique physicochemical properties, including high water solubility, tunable viscosity, and excellent compatibility with biomolecules, making it particularly suitable for the formation of ATPSs [14,15].

The formation of ATPSs by combining PEG with ionic liquids (ILs) is enabled by ILs' unique properties, including high separation efficiency, thermal and chemical stability, recyclability, and tunable physicochemical properties [16,17]. In 2012, the introduction of choline-based ILs—more biocompatible and less toxic than imidazolium-based ones—expanded the biotechnological applications of ATPSs [2]. More recently, polyethylene glycol methyl ether (PEGME 550) has been proposed due to its high solubility, low toxicity, and biocompatibility [18]. Its ether groups promote hydrogen bonding, influencing phase separation and solute partitioning, while the terminal methoxy group enhances tunability and protein selectivity compared to conventional PEGs. These features make PEGME 550 particularly suitable for biomolecule separation under mild conditions, preserving protein structure and activity [19–20].

ATPSs based on choline-derived ionic liquids and polymers are widely used for protein partitioning due to their easy phase formation. Santos et al. [21] formed ATPSs with choline-based ILs and acetonitrile for capsaicin purification. Similarly, systems combining choline-based ILs with PPG 400 enabled BSA partitioning into the IL-rich phase and IgG purification from rabbit serum [22]. Overall, ATPSs are versatile platforms for separating proteins of pharmaceutical, chemical, and food interest [23].

BSA is widely used as a model protein due to its well-characterized physicochemical properties and biological relevance, including roles in transport, detoxification, and antioxidant activity [24]. It is a stable protein composed of 583 amino acids, 17 disulfide bonds, and a molecular weight of 66.4 kDa [25]. In contrast,

immunoglobulin G (IgG) is a polyclonal antibody produced by plasma cells that plays a central role in the immune system. Beyond directly recognizing and neutralizing antigens, IgG activates the complement system, contributing to key defense mechanisms such as inflammation and phagocytosis [26]. Investigating IgG partitioning in ATPS is therefore highly relevant, particularly for purification processes, as IgG is one of the most abundant and biologically important antibody classes. Its broad applicability in disease diagnosis, therapeutic development, and vaccine production further highlights its biotechnological and pharmaceutical importance [27].

In this context, novel ATPSs composed of choline-based ILs and PEGME 550 were developed to evaluate their applicability for the extraction of BSA as a model protein and, subsequently, IgG. Molecular docking simulations were employed to investigate the interactions between the anions and cation of the choline-based ILs and the proteins, providing mechanistic insights into the partitioning behavior observed in the studied ATPSs. Emphasis was placed on assessing the structural stability of these biomolecules after the partitioning process within the proposed systems.

2. Material and Methods

2.1. Material

Polyethylene glycol methyl ether 550 g $gmol^{-1}$ (90 wt% pure) and choline-based ionic liquids (choline bitartrate - [Ch][BIT], choline dihydrogen citrate - [Ch][DHC], and choline chloride – [Ch]Cl), all with purities above 98 wt%, were acquired by Sigma-Aldrich and used for the determination of the phase diagrams. The synthetized choline 2-[4-(2-hydroxyethyl)piperazin-1-yl]ethane-1-sulfonate - [Ch][HEPES] (purity > 99.5 wt%), was synthesized by us [28]. Detailed information on the ATPS constituents is presented in Table 1.

Table 1. Information on the ATPS constituents

Constituent	Abbreviation	Supplier	CAS Reg. no	Chemical Structure	Mass Fraction Purity (wt%)
Polyethylene glycol methyl ether 550	PEGME 550	Sigma-Aldrich	9004-74-4	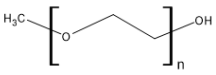	> 90
Choline bitartrate	[Ch][BIT]	Sigma-Aldrich	87-67-2	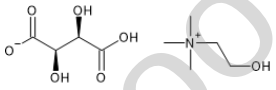	> 98
Choline dihydrogen citrate	[Ch][DHC]	Sigma-Aldrich	77-91-8	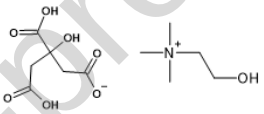	> 98
Choline chloride	[Ch]Cl	Sigma-Aldrich	67-48-1	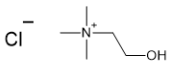	> 98
Choline HEPES	[Ch][HEPES]	Synthesized by us		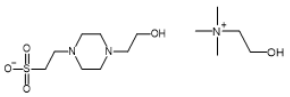	> 99.5

Protein partitioning studies were carried out using bovine serum albumin (BSA) at 90 wt% purchased from INLAB as the model protein. Sheep serum immunoglobulin G (IgG) ≥ 95 wt% was acquired from Sigma-Aldrich. All other reagents were of analytical grade, and ultrapure water was produced by double distillation followed by reverse osmosis (Milli-Q Plus 185).

2.2. Phase Diagram

The solubility (binodal) curves were determined by cloud-point titration at 298 ± 1 K and 0.10 ± 0.01 MPa, a procedure widely employed by our research group [29,30]. An aqueous solution of the choline-based ionic liquid (75 wt%) was added dropwise to a 10 mL tube containing pure PEG methyl ether 500 (PEGME 500, 100 wt%) until the onset of turbidity, indicating phase separation (biphasic region). Subsequently, ultrapure water was added dropwise until the system became completely transparent, corresponding to the monophasic region. This procedure was repeated to obtain enough

experimental data points for constructing the binodal curve. The composition of each system was determined gravimetrically by quantifying all added components using an analytical balance (Shimadzu AUW220D) with an uncertainty of ± 1.0 × 10^{-4} g. The experimental data were fitted using Equation (1) proposed by Merchuk et al. [31].

$$[PEGME] = A\exp[(B[IL]^{0.5}) - (C[IL]^{3})] \quad (1)$$

where [PEGME] and [IL] are the mass fractions of PEGME 550 and ionic liquid, respectively. A, B, and C are the adjusted parameters obtained by non-linear regression. The parameters of this equation are empirical and lack a direct physicochemical interpretation.

Two mixture points were selected within the biphasic region for all systems, and the corresponding tie lines (TLs) were determined. Briefly, the appropriate amounts of each constituent were weighed gravimetrically, thoroughly mixed by vigorous stirring, and subsequently centrifuged (Centrilab 80-2B) at 2,000 rpm for 10 min to accelerate phase separation. The systems were then allowed to equilibrate in a thermostatic bath at 298 K and 0.10 ± 0.01 MPa for 4 h. Upon reaching equilibrium, the bottom phase was carefully withdrawn using a syringe fitted with a long needle. At the same time, the top phase was collected using a pipette. The masses and volumes of the coexisting phases were measured and used to calculate the phase compositions by solving Equations (2–5), applying the lever rule method.

$$[PEGME]_T = A\exp[(B[IL]_T^{0.5}) - (C[IL]_T^{3})] \quad (2)$$

$$[PEGME]_B = A\exp[(B[IL]_B^{0.5}) - (C[IL]_B^{3})] \quad (3)$$

$$[PEGME]_T = \frac{[PEGME]_M}{\alpha} - \frac{1-\alpha}{\alpha}\ [PEGME]_B \quad (4)$$

$$[IL]_T = \frac{[IL]_M}{\alpha} - \frac{1-\alpha}{\alpha}\ [IL]_B \quad (5)$$

where the subscripts M, T, and B denoting the mixture point, top, and bottom phases, respectively, and α corresponds to the ratio between the mass of the top phase and the total weight of the mixture.

The tie-line lengths (TLLs) were determined according to Equation (6),

$$TLL = \sqrt{([PEGME]_T - [PEGME]_B)^2 + ([IL]_T - [IL]_B)^2} \quad (6)$$

2.3. Partitioning/Extraction of Proteins

Initially, the mixture point with the largest biphasic area (45 wt% PEGME 550 and 40 wt% IL) was used to study the partitioning of BSA (1 mg mL^{-1}) as a model protein. The constituents were vigorously stirred, centrifuged at 2,000 rpm, and left in a thermostatic bath at 298 ± 1 K and 0.10 ± 0.01 MPa for 4 h. After the separation of coexisting phases, the volume and mass were determined, and protein concentration was measured by Bradford's method [32]. Protein concentrations were determined in triplicate, and the results are expressed as mean ± standard deviation. For the IgG partitioning, the ATPS composition with the best stability for the protein model was chosen. In this case, the effects of PEGME 550 (35–50 wt%) and IL (30–45 wt%) concentrations, as well as temperature (298–318 K), on IgG partitioning were investigated.

For all systems, the partition coefficient of proteins (K), volumetric ratio (R_V), and extraction efficiency (EE%) were determined according to Equations (7–9).

$$K = \frac{[C_T]}{[C_B]} \quad (7)$$

$$R_V = \frac{V_T}{V_B} \quad (8)$$

$$[EE]_B\% = \frac{K100}{1+R_V K} \quad (9)$$

where C corresponds to BSA or IgG concentration, V is the volume of the phase, and the subscripts T and B represent the top and bottom phases, respectively.

The van't Hoff equation was used to determine the standard molar thermodynamic functions of transfer such as Gibbs free energy of transfer ($\Delta_{tr}G^o_m$), the standard molar enthalpy of transfer ($\Delta_{tr}H^o_m$) and standard molar entropy of transfer ($\Delta_{tr}S^o_m$), correlated with the IgG partition coefficient at different temperatures (298 a 318 K), as described in the Equations (10–12).

$$\Delta_{tr}G^o_m = -RTln(K) \quad (10)$$

$$ln(K) = \frac{\Delta_{tr}H^o_m}{R}\frac{1}{T} + \frac{\Delta_{tr}S^o_m}{R} \quad (11)$$

$$\Delta_{tr}G^o_m = \Delta_{tr}H^o_m - T\Delta_{tr}S^o_m \quad (12)$$

where T is temperature (Kelvin), and R is the ideal gas constant. The enthalpy and entropy contributions can be directly deduced from the linear approximation of ln(K) versus T^{-1}.

2.4. Protein Stability

The analysis of protein stability was performed by evaluating the secondary structure changes of each protein using Fourier transform infrared (FTIR) spectroscopy (Cary 630 FTIR spectrometer - Agilent Technologies) before and after the partitioning process in ATPS formed by PEGME 550 (45 wt%) + IL (40 wt%) + protein aqueous solution (15 wt%). The FTIR was equipped with an attenuated total reflection (ATR) sampling unit. The spectra were recorded in transmittance mode between 500 and 4,000 cm^{-1} with a resolution of 4 cm^{-1} and 32 scans. FTIR spectra were performed in the amide I region (1700–1600 cm^{-1}), identifying peak frequencies through secondary derivative analysis and deconvoluted peaks using Origin 8.5 software.

2.5. Molecular Docking

Molecular docking simulations between BSA and IgG with ILs, including both cations and anions, were performed using the AutoDock Vina 1.1.2 program [33]. The three-dimensional atomic coordinates of the ILs (ligands) were generated using Discovery Studio, v20 (Accelrys, San Diego, CA, USA). Ligand rigid roots were defined using AutoDockTools (ADT), setting all possible rotatable bonds as active by torsions [34]. Receptor structures for BSA (PDB ID: 4f5s) and IgG (PDB ID: 1igt) were prepared by removing chain B from BSA and the light chains from the IgG. Non-polar hydrogen atoms were merged, and partial atomic charges and atom types were assigned using AutoDockTools (ADT). The grid box was centered at the center of mass of each receptor (x-, y-, and z-axes). For BSA, the grid was 8.437 Å × 21.632 Å × 106.577 Å, while for IgG, it was 3.917 Å × -37.056 Å × 31.389 Å. The grid dimensions were set to 98 Å × 78 Å × 96 Å for BSA, and 72 Å × 72 Å × 62 Å for IgG. For each ligand (IL cations and anions considered individually), the binding modes were explored by generating and evaluating 10 distinct docking conformations.

2.6. SDS-PAGE Gel Electrophoresis

The SDS-PAGE protein analysis was performed using a vertical slab apparatus, the Mini-PROTEAN Tetra System (Bio-Rad, Brazil), with 12% resolving gels and 4% stacking gels at pH 8.8, following the method of Laemmli [35]. The electrophoretic

process lasted 15 min at 90 V and 40 min at 180 V. Proteins were visualised by staining with an ethanolic solution of Coomassie blue (0.25 wt%). Protein markers, purchased from Sigma-Aldrich, contained aprotin (6.5 kDa), a-lactalbumin (14.2 kDa), trypsin inhibitor (20.1 kDa), trypsinogen (24.0 kDa), carbonic anhydrase (29.0 kDa), glyceraldehyde-3-phosphate dehydrogenase (36.0 kDa), ovalbumen (45.0 kDa), and albumin (66.0 kDa), and were separated on stacking gels at pH 8.8.

2.7. Statistical Analysis

Protein concentrations were measured in at least triplicate, and the results are expressed as mean ± standard deviation. The data were statistically evaluated using one-way analysis of variance (ANOVA), followed by Tukey's post hoc test for multiple comparisons. Differences were considered statistically significant at $p \leq 0.05$.

3. Results and Discussion

3.1. Phase Diagram

Figure 1 (detailed data in Tables S1–S4 in the Supporting Information) depicts the binodal (solubility) curves of the novel ATPSs composed of PEGME 550, choline-based ILs, and water, which were obtained at 298 ± 1 K and 0.10 ± 0.01 MPa. The binodal curves are expressed in molality units to avoid misinterpretation arising from differences in the molecular weights of the system constituents, being defined as the molality of PEGME 550 per kilogram of solvent (water + IL) versus the molality of IL per kilogram of solvent (water + PEGME 550). Analysis of the phase diagrams allowed assessment of the IL ability to induce ATPS formation, as indicated by the area above the binodal curve corresponding to the biphasic region, which is directly related to the easiness of phase separation. The remaining curves are presented as weight percentages to facilitate the interpretation of the selected compositions used for system preparation, being this more useful to address the protein partitioning studies and potential application.

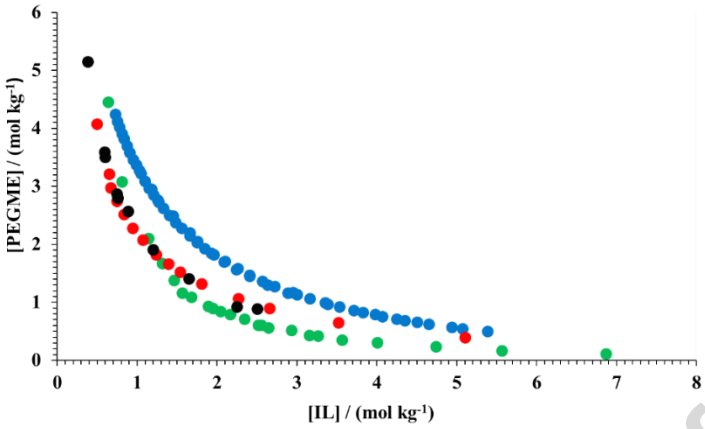

Figure 1. Phase diagram of ATPS based on PEGME 550 + IL + water at 298 ± 1 K and 0.10 ± 0.01 MPa. [Ch]Cl - ●, [Ch][DHC] - ●, [Ch][HEPES] -● and [Ch][BIT] - ●.

According to Pereira et al. [19], phase formation in polymer–IL-based ATPSs depends on the hydrogen-bond donor/acceptor interactions among the polymer, water, and IL. In this context, the hydroxyl group of PEGME 550 acts as a hydrogen-bond donor, while the IL anions act as hydrogen-bond acceptors [36]. Consequently, and given that the cholinium cation is common to all ILs studied, the increase in the hydrogen-bond acceptor amount (values in parentheses) of the IL anions facilitate phase formation, following the order Cl^- (0) < $[HEPES]^-$ (6) ≈ $[BIT]^-$ (6) < $[DHC]^-$ (7). As a result, [Ch]Cl exhibits the weakest interaction capability and, therefore, the lowest salting-out effect.

Similar phase-separation behavior was reported by Santos et al. [21] for ATPSs formed by choline-based ionic liquids and acetonitrile, where the driving force for phase separation was attributed to the hydrophilic–lipophilic balance, as reflected in the octanol–water partition coefficient (log K_{ow}). In that study, the reported values followed the order [Ch][DHC] (−1.32) > [Ch][BIT] (−1.43) >> [Ch]Cl (−3.70), which is consistent with the trend observed in the present work. It is also important to highlight that systems based on organic solvents may pose limitations regarding protein stability. For instance, although acetonitrile is widely used in analytical chemistry (e.g., HPLC), it may affect protein structure. In contrast, polymers such as PEG and their ether derivatives are generally regarded as non-toxic under typical conditions of use, making them more suitable for applications involving sensitive biomolecules.

The experimental binodal data were fitted using Equation (1), where the parameters A, B, and C were estimated by least-squares regression. The mean value, standard deviation, and regression coefficient (R^2 = 0.997 < R^2 < 0.999) are shown in

Table 2. Additionally, the tie-lines obtained from Equations (2–5) are presented in Figure 2. The compositions of the mixture points and of the coexisting phases, as well as the lengths of the tie-lines, are provided in Table 3.

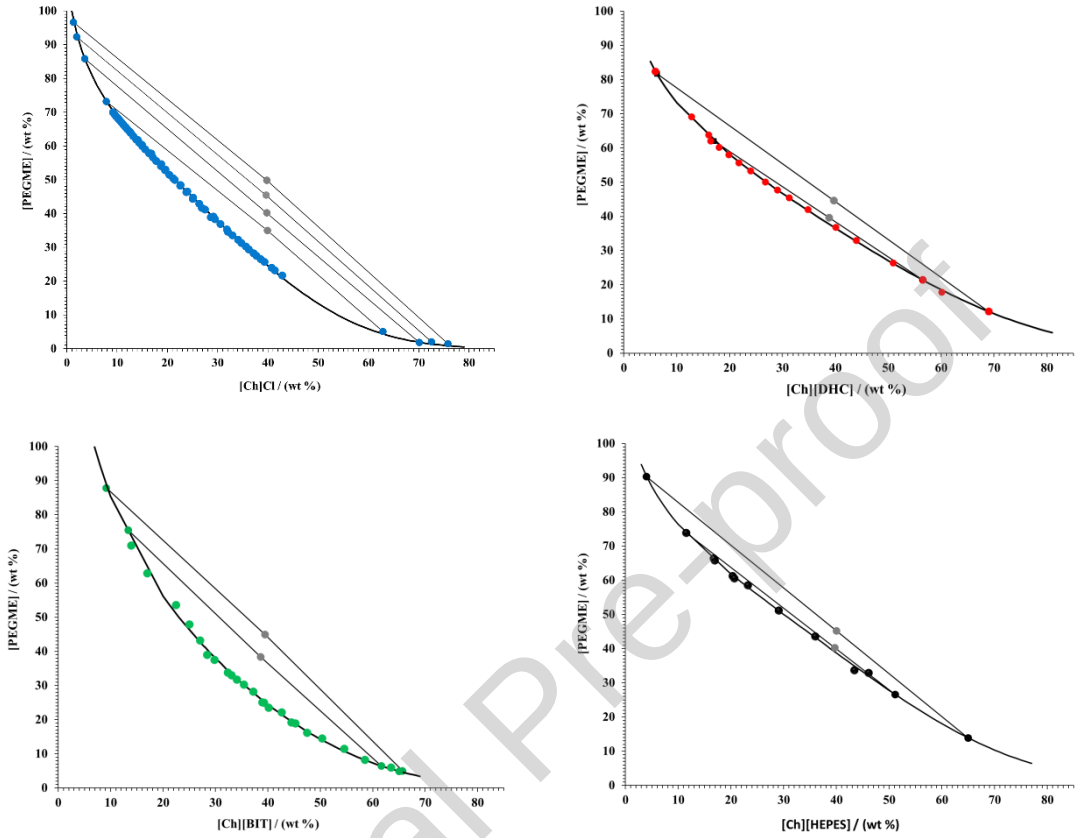

Figure 2. Phase diagrams, including the tie-lines, of ATPSs formed by PEGME 550 + IL + water at 298 ± 1 K and 0.10 ± 0.01 MPa. [CH]Cl- ●; [CH][BIT]- ●; [CH][HEPES]- ●; [CH][DHC]- ●.

Table 2. Regression parameters and standard deviation of equation (1) for ATPSs formed by PEGME 550 + IL + water at 298 ± 1 K and 0.10 ± 0.01 MPa.

IL	Regression Parameters			R^2
	(A ± σ)	(B ± σ)	10^{-6}(C ± σ)	
[Ch]Cl	118.3 ± 0.9	-0.169 ± 0.002	7.9 ± 0.1	0.999
[Ch][BIT]	216 ± 1	-0.29 ± 0.01	5.2 ±0.4	0.997
[Ch][DHC]	122 ± 3	-0.161 ± 0.005	2.9 ± 0.2	0.999
[CH][HEPES]	120 ± 4	-0.141 ± 0.009	3.7 ± 0.4	0.998

Table 3. Mass composition for the tie-lines (TLs) and respective tie-line lengths (TLLs) for ATPSs composed of IL + PEGME 550 + H_2O at 298 K and 0.1 MPa.[a]

IL	Mass Composition (wt%)									TLL
	[PEGME]$_M$	[IL]$_M$	[H_2O]$_M$	[PEGME]$_T$	[IL]$_T$	[H_2O]$_T$	[PEGME]$_B$	[IL]$_B$	[H_2O]	
[Ch]Cl	34.97	39.92	25.11	73.21	7.80	18.99	5.12	62.83	32.05	103.54
	40.23	39.74	20.03	85.94	3.55	10.51	1.91	70.06	28.03	107.16
	45.45	39.63	14.92	92.44	1.95	5.61	2.13	72.50	25.37	121.45
	49.83	39.80	10.37	96.69	1.29	2.02	1.54	75.74	22.72	129.69
[Ch][DHC	39.59	38.83	21.58	62.07	16.97	20.96	21.39	56.51	22.10	56.73
	44.67	39.68	15.65	81.76	6.22	12.02	12.19	68.96	18.85	93.68
[Ch][BIT]	38.42	38.62	22.96	75.57	13.31	11.12	6.46	61.61	31.93	82.68
	44.99	39.42	15.59	87.91	9.12	2.97	5.06	64.63	30.31	106.26
[Ch][HEP]	40.24	39.72	20.04	73.92	11.43	14.65	26.60	51.16	22.24	61.79
	45.16	40.03	14.81	90.24	4.03	5.73	13.90	64.99	21.11	67.66

[a] Standard uncertainties u is u([PEGME], [IL] or [water]) = 0.01, u(T) = 1 K, and u(p) = 10 kPa.

3.2. Partitioning and Stability of Bovine Serum Albumin

BSA was selected as a model protein due to its wide availability, low cost, high-water solubility, and well-characterized molecular structure [37,38]. These features make BSA a standard reference protein for preliminary evaluation of the performance and applicability of ATPSs in partitioning processes. The primary objectives were to investigate the structural stability and behavior of BSA in the presence of the constituent ILs and to establish a robust methodology for other relevant separations. For this purpose, each ATPS was prepared with a fixed mass composition, consisting of 45 wt% PEGME, 40 wt% of each IL, and 15 wt% of water containing BSA (1 mg mL^{-1}). The partitioning parameters, namely the partition coefficient (K) and extraction efficiency (EE%), were determined for each system, whose results are presented in Figure 3 (Table S5 in the Supporting Information provides the detailed data).

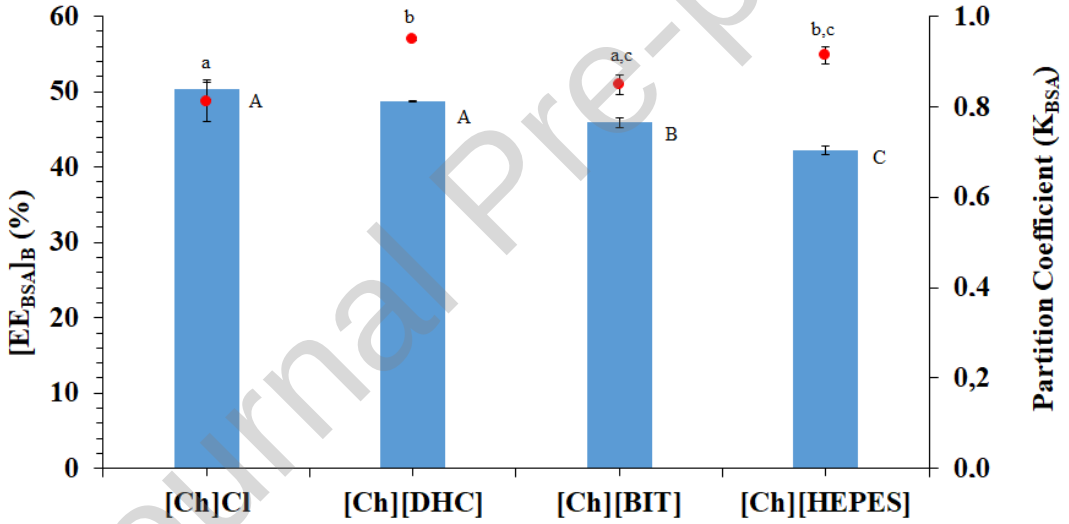

Figure 3. Partition coefficient (K_{BSA}) (●) and extraction efficiency $[EE_{BSA}]_B$ (■) of BSA in the bottom phase (IL-rich) of ATPSs composed of PEGME 550 (45 wt%) and cholinium-based ILs (40 wt%) at 298 K and 0.1 MPa. Means followed by the same letter (lowercase for K_{BSA} and uppercase for $[EE_{BSA}]_B$) do not differ significantly according to Tukey's test ($p \geq 0.05$)

The protein partitioning mechanism in ATPSs is a highly complex process governed by multiple physicochemical factors, among which the hydrophilicity of the IL anion plays a decisive role. In IL-based ATPSs, electrostatic interactions between charged amino acid residues and IL ions, together with hydrogen-bonding interactions involving

polar protein domains, water molecules, and IL components, constitute the main driving forces controlling protein distribution between the coexisting phases. Variations in anion hydration ability significantly influence protein solvation, stability, and affinity toward each phase, ultimately determining partition coefficients and extraction efficiencies [39-41].

All investigated systems were able to partition BSA without any evidence of protein precipitation at the interface of the coexisting phases. The partition coefficient values ($K < 1.0$) obtained for all systems indicate a preferential partitioning of the model protein toward the bottom phase, which is predominantly enriched in the IL. Since all systems share the same cholinium cation, differences in protein partitioning primarily reflect the nature of the IL anions and their ability to form hydrogen-bonding interactions with water molecules and polar amino acid residues on the BSA surface [42]. An exception was observed for the system containing [Ch][HEPES], which exhibited a partition coefficient close to unity ($K_{BSA} = 0.91$). This behavior may be associated with specific π–π interactions between the imidazolium-like aromatic moiety of the HEPES-based anion and aromatic amino acid residues present in the BSA structure, leading to a more balanced distribution of the protein between the two phases [36,43]. The most favorable partitioning towards the IL-rich phase is indicated by the lowest KBSA values, which were observed for the systems containing [Ch]Cl (0.81 ± 0.04) and [Ch][BIT] (0.85 ± 0.02), which are statistically similar at a 95% confidence level ($p < 0.05$). In addition, the $[EE_{BSA}]_B$ follows the same trend as the log Kow values of the cholinium-based ionic liquids, suggesting that the hydrophilic–lipophilic balance of the ILs plays a key role in governing protein partitioning. The best values were observed for [Ch]Cl (50.31 ± 1.30 %) and [Ch][DHC] (48.71 ± 0.10 %), which were statistically similar ($p > 0.05$), indicating that these ILs allow more protein to be extracted into the IL-rich phase. The best extraction condition was achieved with [Ch]Cl, as it exhibited the lowest K_{BAS} values and the highest $[EE_{BSA}]_B$.

Molecular docking simulations were employed to investigate the mechanism underlying BSA partitioning in ATPSs with ILs. This approach allowed the identification of preferential interactions between IL ions and specific residues on the protein surface. The results (Table S6 and Figures S1-S2 in the Supporting Information) revealed that, except for Cl^-, IL anions exhibited more negative binding free energy values than the $[Ch]^+$ cation, indicating stronger interactions with BSA. However, a stronger binding

affinity did not directly translate into a higher extraction efficiency, highlighting the importance of the interaction type and reversibility for effective protein partitioning.

The $[Ch]^+$ cation displayed limited affinity, forming only a single hydrogen bond with Thr44, suggesting limited affinity toward the protein surface. Among the anions, $[BIT]^-$ displayed multiple hydrogen bonds with Asp108, Tyr147, and Lys465, promoting favorable yet reversible interactions that correlate with moderate extraction efficiency. In contrast, $[HEPES]^-$ and $[DHC]^-$ engaged in several electrostatic interactions in addition to hydrogen bonding, primarily involving arginine and alanine residues. $[HEPES]^-$ interacted through a combination of hydrogen bonding and electrostatic interactions with residues Arg208 and Ala209, indicating contributions from both electrostatic and hydrophilic interactions. In addition, $[DHC]^-$ exhibited a more complex anchoring pattern, involving several electrostatic interactions and hydrogen bonds with Arg198, Arg217, Arg256, and Ala290. Hydrogen bonds were observed at short distances (1.93–3.00 Å), while electrostatic interactions occurred at distances greater than 4.00 Å. Overall, these findings indicate that effective BSA partitioning in ATPSs is governed not solely by binding affinity, but by the nature and reversibility of protein–IL interactions. ILs with moderate hydrogen-bonding interactions, such as [Ch]Cl and [Ch][BIT], have a more efficient extraction. In contrast, ILs dominated by strong electrostatic interactions, such as [Ch][HEPES] and [Ch][DHC], promote protein migration toward the opposite phase.

This partitioning trend is consistent with observations reported in previous studies, in which BSA preferentially partitioned into IL-rich phases in systems composed of PEGDME-250 and cholinium-based ILs [45,46]. In addition, other ATPSs incorporating cholinium-based ILs, such as [Ch][Pro], [Ch][Lac], [Ch][Ben], [Ch][Cit], and [Ch][Glyco], in combination with polymeric phase-forming agents, have also demonstrated effective BSA partitioning and purification toward the IL-enriched phase [2].

In addition to molecular interaction analyses, the structural behavior of BSA in media containing salts and chemical constituents was evaluated to elucidate possible changes in its conformational stability. For this purpose, FTIR spectra were obtained recorded for standard BSA, BSA in water, and BSA in the presence of each IL investigated, allowing the identification of characteristic bands and functional groups associated with each system (Figure 4).

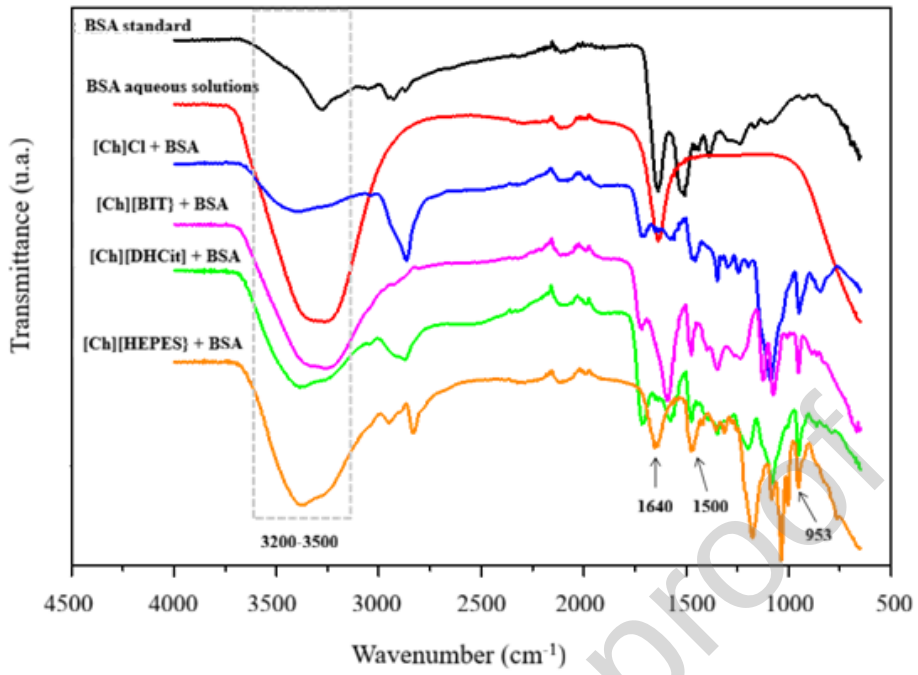

Figure 4. FTIR spectra of BSA: standard BSA (—), aqueous BSA solution (—), and bottom phases of ATPSs containing BSA and cholinium-based ILs: [Ch]Cl (—), [Ch][BIT] (—), [Ch][DHC] (—), and [Ch][HEPES] (—).

The FTIR spectra exhibited multiple absorption bands, with particular emphasis on the high-wavenumber region (2500–4000 cm^{-1}). Stretching vibrations observed in the 3200–3500 cm^{-1} range — absent only in the standard BSA spectrum — were attributed to O–H groups and water molecules, confirming the high moisture content of the samples [47]. All spectra displayed the characteristic bands of BSA, notably the amide I band (1600–1700 cm^{-1}, C=O stretching) and the amide II band (~1500 cm^{-1}, C–N stretching), confirming the preservation of the protein backbone structure [48]. The presence of C–C–O stretching vibrations at approximately 953 cm^{-1}, attributed to the $[Ch]^+$ cation, was observed in all IL-containing systems. This finding indicates that, despite the coexistence of amide I and II bands and the formation of protein–IL interactions, the cholinium structure remains intact, showing no significant band shifts or vibrational changes. Moreover, these bands confirm the presence of the ILs in the bottom phase of the systems [49]. Possible conformational changes in BSA were further investigated by spectral deconvolution of the amide I region (1600–1700 cm^{-1}), which enabled quantitative assessment of secondary structure elements, including α-helix, β-sheet, β-turn, and random coil (Figure 5).

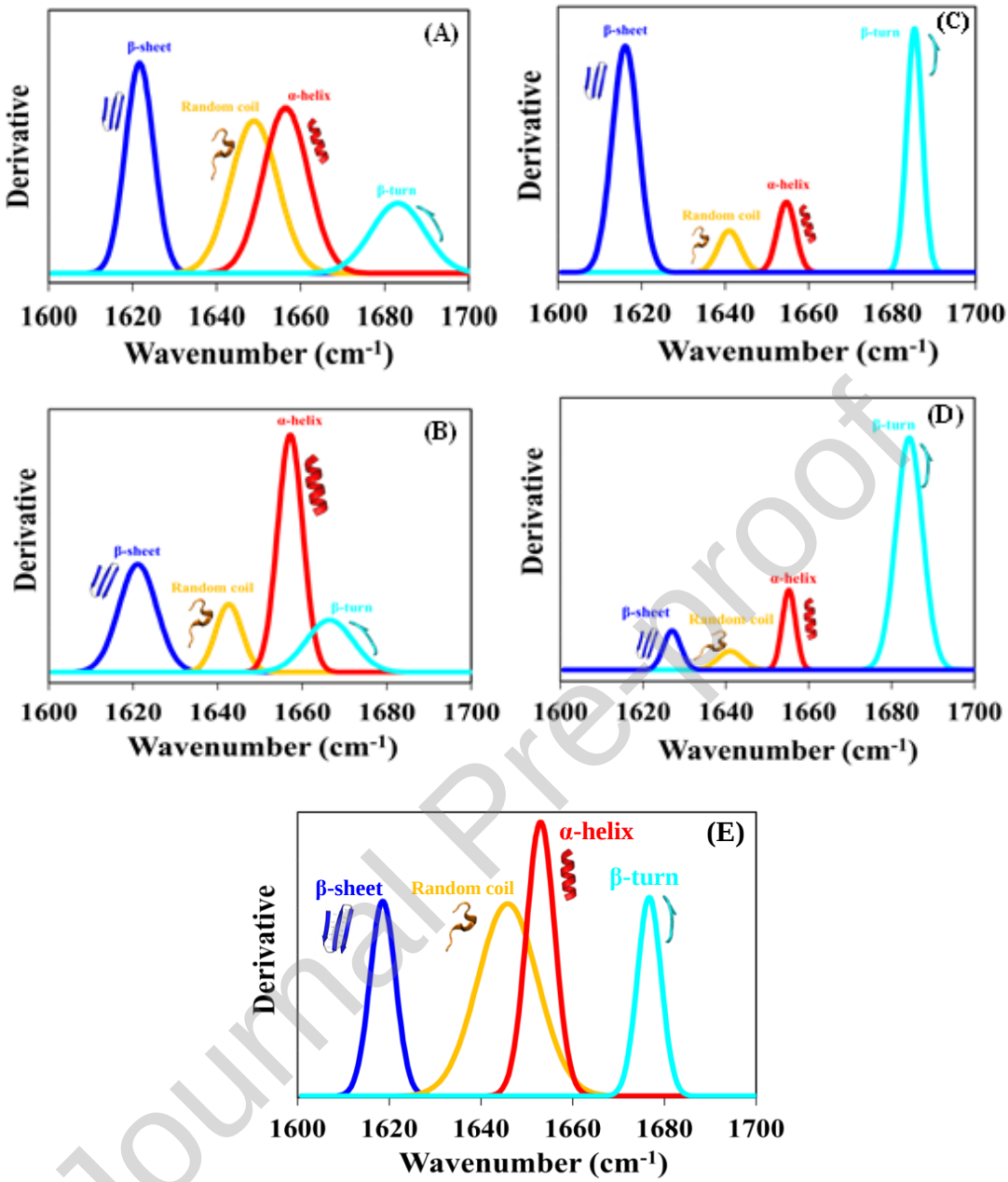

Figure 5. Deconvoluted FTIR (secondary-derivative) spectra in the Amide I region (1,700–1,600 cm^{-1}) of BSA in different solvents: (A) aqueous solution (model system); (B) [Ch]Cl; (C) [Ch][BIT]; (D) [Ch][DHC]; and (E) [Ch][HEPES].

The deconvoluted spectra shown in Figure 5 (C and D) revealed an increased exposure of β-structure content in the presence of the ILs [Ch][BIT] and [Ch][DHC], with a more pronounced effect observed for $[DHC]^-$. This behavior suggests that interactions between the hydrophobic regions of BSA and the IL anions are dominant, particularly for $[DHC]^-$, whose strong electrostatic interactions, combined with a reduced capacity for hydrogen bonding, may contribute to partial protein destabilization. These findings are

consistent with previous studies [50], which associate an increase in β-sheet content with the conversion of α-helical structures into β-conformations, a process often linked to protein fibrillation and precipitation phenomena. According to Shmoo et al. [51], [Ch][DHC] exhibits the highest stabilizing effect, whereas [Ch]Cl shows the weakest. Therefore, it is crucial to identify the most suitable cholinium-based ionic liquid before performing partitioning studies with IgG.

In contrast, the presence of [Ch]Cl (Figure 5B) led to an increase in the α-helical content of BSA. This effect can be attributed to the small size and high charge density of the chloride anion, which favors interactions with the protein hydration shell. Such interactions may promote the rearrangement of internal hydrogen bonds, leading to an expansion and enhancement of the spectral features characteristic of α-helical structures. Similarly, the [Ch][HEPES] system (Figure 5E) also exhibited an increase in α-helical content, albeit to a lesser extent. This observation indicates that the $[HEPES]^-$ anion interacts with the protein in a more distributed manner, leading to a balanced structural reorganization. The relatively high α-helix content of [Ch]Cl and [Ch][HEPES] suggests that only minor conformational perturbations occur, preserving the overall structural integrity and functional stability of BSA [25, 52-54].

3.2. Partitioning and Stability of Immunoglobulin G

Based on the preceding results, [Ch]Cl was selected for proceeding the study due to its lower partition coefficient, higher protein extraction efficiency in the bottom phase, and the promising structural stability of the model protein BSA. The optimal conditions for IgG partitioning were subsequently investigated using the proposed system composed of PEGME 550 (35, 40, 45, and 50 wt%), [Ch]Cl (30, 35, 40, and 45 wt%), evaluated over a temperature range of 298–318 K at 0.1 MPa. The results of the IgG partitioning experiments under these conditions are presented in Tables 4–6.

Initially, the effect of PEGME 550 concentration was investigated in ATPSs composed of PEGME 550, [Ch]Cl (40 wt%), and water at 298 K and 0.1 MPa, as summarized in Table 4.

The results demonstrated that the concentration of PEGME 550 strongly influenced IgG partitioning behavior. In systems containing 35–45 wt% of the polymer, IgG preferentially partitioned into the bottom phase, which is enriched in [Ch]Cl. However, a critical increase to 50 wt% PEGME 550 led to a complete inversion of partitioning, driving IgG toward the top or polymer-rich phase. This transition can be

attributed to a shift in the balance of forces governing protein partitioning. According to Spelzine et al. [55], the partitioning of medium- to high-molecular-weight proteins can be controlled by either specific interactions and affinities between the macromolecule and the surrounding medium or by excluded-volume effects. Up to 45 wt% PEGME, the salting-out effect induced by [Ch]Cl in the bottom phase is the dominant driving force, overcoming the moderate excluded-volume effects present in the polymer-rich phase and resulting in partition coefficients lower than unity ($K < 1$). At 50 wt% PEGME, however, the system reaches a critical threshold at which the adequate excluded volume in the top phase increases sharply and nonlinearly. Under these conditions, the high degree of chain entanglement and increased polymer density generate a sterically restrictive environment, making the presence of the large IgG macromolecule energetically unfavorable. Consequently, the steric exclusion force surpasses the salting-out effect, reversing the system selectivity and yielding partition coefficients greater than unity ($K > 1$). This behavior underscores the crucial role of polymer concentration in regulating the partition equilibrium of high-molecular-weight proteins in ATPSs [22,36,56]. All K_{IgG} and $[EE_{IgG}]_B$ values differ significantly from one another at the 95% confidence level ($p \leq 0.05$).

Table 4. Partition coefficient (K_{IgG}) and extraction efficiency $[EE_{IgG}]_B$ of IgG in ATPSs composed of PEGME 550 + [Ch]Cl (40 wt%) + water at 298 K and 0.1 MPa.

[PEGME 550] (wt%)	**K_{IgG}**	**$[EE_{IgG}]_B$ (%)**
35	0.87 ± 0.01^{a}	32.9 ± 0.2^{A}
40	0.83 ± 0.01^{b}	34.1 ± 0.6^{B}
45	0.70 ± 0.01^{c}	48.68 ± 0.33^{C}
50	1.155 ± 0.003^{d}	46.30 ± 0.06^{D}

Means followed by the same letter (lowercase for K_{IgG} and uppercase for $[EE_{IgG}]_B$)) do not differ significantly according to Tukey's test ($p \geq 0.05$)

Based on these findings, the condition containing 45 wt% PEGME 550 was selected for subsequent studies, as it represents the optimal operating point, combining high IgG recovery in the bottom phase ($K_{IgG} = 0.70$) with robust system stability, while remaining below the phase-inversion threshold observed at higher polymer concentrations. With the PEGME 550 concentration fixed at its optimal value (45 wt%), the effect of the ionic liquid [Ch]Cl concentration on IgG partitioning was systematically

investigated at 298 K and 0.1 MPa. The [Ch]Cl content ranged from 30 to 45 wt%, with the corresponding results summarized in Table 5.

Table 5. Partition coefficient (K_{IgG}) and extraction efficiency $[EE_{IgG}]_B$ of IgG in ATPSs composed of PEGME 550 (45 wt%) + different concentrations of [Ch]Cl + water at 298 and 0.1 MPa.

[Ch]Cl (wt%)	K_{IgG}	$[EE_{IgG}]_B$ (%)
30	0.80 ± 0.02^{a}	34.9 ± 0.6^{A}
35	0.78 ± 0.04^{a}	46.3 ± 0.9^{B}
40	0.70 ± 0.01^{b}	48.68 ± 0.33^{C}
45	1.364 ± 0.001^{c}	42.30 ± 0.01^{D}

Means followed by the same letter (lowercase for K_{IgG} and uppercase for $[EE_{IgG}]_B$)) do not differ significantly according to Tukey's test ($p \geq 0.05$)

The migration behavior of IgG changed markedly with increasing concentrations of the system constituents. At lower concentrations, the protein preferentially partitioned into the bottom phase of the systems. However, when the concentration exceeded 40 wt%, IgG migration shifted toward the top phase, resulting in higher values of both K_{IgG} and $[EE_{IgG}]_B$. This behavior can be attributed to a reduction in protein solubility in the bottom phase as the ionic liquid concentration increases, in agreement with the finding of Barbosa et al. [57]. The higher ionic strength enhances the salting-out effect, weakening protein–solvent interactions in the IL-rich phase and promoting protein migration toward the polymer-rich phase. Consequently, this salting-out-driven mechanism becomes the dominant force governing IgG partitioning at higher concentrations of ionic liquid. The K_{IgG} and $[EE_{IgG}]_B$ values differ significantly from one another ($p \leq 0.05$), except the K_{IgG} at 30 and 35% of [[Ch]Cl, which are statistically similar.

Considering the optimal partitioning conditions, defined by the lowest K_{IgG} value and the highest $[EE_{IgG}]_B$, namely PEGME 550 (45 wt%) + [Ch]Cl (40 wt%) + water (15 wt%) at 298 K and 0.1 MPa, the effect of temperature on IgG partitioning was evaluated at 298, 303, 308, 313, and 318 K. The corresponding results are provided in Table 6.

Table 6. Partition coefficient (K_{IgG}) and extraction efficiency ($[EE_{IgG}]_B$) of IgG in ATPSs composed of PEGME 550 (45 wt%) + [Ch]Cl (40 wt%) + water (15 wt%) at different temperatures and 0.1 MPa.

Temperature (K)	K_{IgG}	$[EE_{IgG}]_B$ (%)
298	0.70 ± 0.01^{a}	48.68 ± 0.33^{A}
303	$0.76 \pm 0.06^{a,b}$	45.13 ± 0.01^{B}
308	$0.78 \pm 0.07^{a,b}$	$46.17 \pm 2.24^{A,B,C}$
313	0.789 ± 0.005^{b}	$45.81 \pm 0.15^{C,D}$
318	0.85 ± 0.04^{c}	$43.92 \pm 1.15^{B,D}$

Means followed by the same letter (lowercase for K_{IgG} and uppercase for $[EE_{IgG}]_B$) do not differ significantly according to Tukey's test ($p \geq 0.05$)

The literature consistently highlights temperature as a crucial parameter influencing biomolecule partitioning in ATPSs [40, 58,59]. The results demonstrate that K_{IgG} exhibits a direct and positive dependence on temperature, increasing from 0.70 at 298 K to 0.85 at 318 K. This behavior can be attributed to the increase in thermal energy, which promotes the migration of IgG from the lower phase (ionic liquid-rich) to the upper phase (polymer-rich), thereby reducing the extraction efficiency of the bottom phase. This trend is consistent with the findings of Zafarani-Moattar et al. [45], who reported a decrease in protein extraction efficiency with increasing temperature, reinforcing that milder conditions are generally more favorable for efficient protein recovery.

The temperature effect may also be associated with changes in protein conformation. Denatured proteins exhibit altered partitioning behavior due to an increased surface area resulting from unfolding and the exposure of hydrophobic residues [41,60]. For instance, BSA preferentially migrates to the IL-rich phase, and its partitioning toward this phase increases with temperature. In addition, elevated thermal energy weakens electrostatic interactions and modifies the hydration of system components, further influencing phase behavior and biomolecule distribution [61,62].

The study was deliberately limited to 318 K, which represents a critical upper threshold for biotechnological applications, as higher temperatures are commonly avoided in protein partitioning processes due to the increased risk of thermal denaturation [63]. IgG inactivation would compromise not only process yield but also the functional integrity of the final product, which is essential for pharmaceutical and diagnostic applications. Therefore, 298 K emerges as the most advantageous temperature, as it

combines higher extraction toward the target phase (IL-rich, K_{IgG} = 0.70) with the preservation of IgG conformational stability and biological activity. It is worth noting that this value is statistically similar to those obtained at temperatures up to 308 K ($p \geq 0.05$), while $[EE_{IgG}]_B$ reaches its highest value ($p \leq 0.05$).

The thermodynamic parameters of the IgG partitioning process, namely the Gibbs free energy change ($\Delta_{tr}G^o_m$), enthalpy change ($\Delta_{tr}H^o_m$), and entropy change ($\Delta_{tr}S^o_m$), were determined from the K_{IgG} values obtained at different temperatures. Table 7 presents the thermodynamic parameters associated with the partitioning of IgG. Van't Hoff's analysis was employed to relate the logarithm of the partition coefficient to the inverse of the absolute temperature. In addition, the Flory-Huggins theory was applied to describe the driving force governing solute partitioning in the system. A linear fit to the experimental data yielded a regression coefficient (R^2) of 0.93, indicating good agreement between the model and the experimental results.

Table 7. Thermodynamic parameters of IgG in ATPSs composed of PEGME 550 (45 wt%) + [Ch]Cl (40 wt%) + water (15 wt%) at different temperatures and 0.1 MPa.

Temperature (K)	$\Delta_{tr}G^o_m$ (kJ mol^{-1})	T.$\Delta_{tr}S^o_m$ (kJ mol^{-1})	$\Delta_{tr}H^o_m$ (kJ mol^{-1})
298.15	568.15	-574.90	
303.15	577.79	-584.54	
308.15	587.44	-594.18	*-6.74*
313.15	597.08	-603.82	
318.15	606.72	-613.46	

From a thermodynamic perspective, a positive Gibbs free energy change ($\Delta_{tr}G°_m > 0$) indicates that the transfer of IgG from its preferred phase (i.e., the ionic liquid-rich bottom phase) to the opposite phase is non-spontaneous, as also reported in the literature [64,65]. Therefore, the protein exhibits a higher affinity for the ionic liquid-rich phase, resulting in a partition coefficient lower than unity ($K_{IgG} < 1$). However, it is important to emphasize that a non-spontaneous transfer does not imply the absence of mass transfer. Rather, it indicates that the equilibrium strongly favors the ionic liquid-rich phase, although a fraction of the protein may still distribute to the other phase. The negative values of $\Delta_{tr}H^o_m$ demonstrate that the process is exothermic, reflecting a favorable enthalpic contribution. However, the strongly negative values of T.$\Delta_{tr}S^o_m$ reveal that IgG partitioning is entropically unfavorable, and this contribution dominates the

thermodynamic balance. Consequently, the process is enthalpically favored but entropy-controlled, becoming less efficient at higher temperatures and more favorable under milder conditions, particularly at 298 K. In this work, the focus was limited to IgG partitioning behavior, and no direct evaluation of contaminant removal was performed. From an industrial perspective, particularly in biopharmaceutical applications, process feasibility is primarily dictated by the purity of the target protein, rather than recovery alone. In many cases, especially for high-value biomolecules such as monoclonal antibodies, achieving a high purification factor is more critical than maximizing recovery in a single step. Moreover, it is well established that, in some systems, the partitioning of the target protein cannot be significantly shifted by adjusting process variables. In such situations, the separation strategy relies instead on the preferential migration of contaminants toward the phase with lower affinity for the target protein. This differential partitioning between the target molecule and impurities increases purification efficiency, even when the target protein remains predominantly in one phase. Nonetheless, the observed thermodynamic tendency suggests that appropriate process optimization could enable efficient separation by driving impurities away from the IgG-enriched phase.

Molecular interaction analyses of IgG were conducted with the same objective established for BSA. The binding modes, interaction types, amino acid residues involved, and interaction distances (Å) between IgG and the constituent ions of [Ch]Cl were systematically determined. Three-dimensional representations of the molecular interactions, highlighting the interacting amino acid residues, are presented in Figure 6 (A and B). In addition, the binding affinities, interacting residues, interaction types, and geometric distances (Å) for [Ch]Cl are summarized in Table S7 of the Supporting Information.

The results demonstrate that the choline cation ($[Ch]^+$) interacts more strongly with the IgG surface, exhibiting a more significant interaction energy than the Cl^- anion. $[Ch]^+$ establishes an electrostatic interaction with an aspartic acid residue at a distance of 5.50 Å. It forms a hydrogen bond with a valine residue at a distance of 2.66 Å. This interaction pattern is consistent with the trends observed for BSA–ionic liquid interactions, confirming that hydrogen-bonding interactions are more distance-sensitive and typically occur at distances of up to 3.0 Å. In contrast, more hydrophobic and electrostatic interactions prevail at distances greater than 4.0 Å [66].

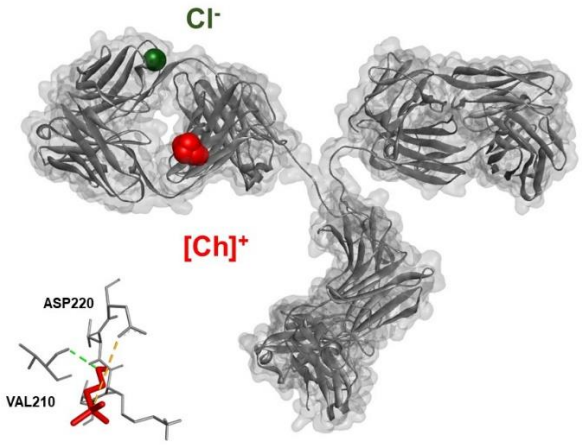

Figure 6. Docking pose with the lowest absolute value of affinity (kcal mol^{-1}) for IgG with $[Ch]^+$ and Cl^- and diagram of the molecular interaction between IgG with $[Ch]^+$.

The stability of IgG during the partitioning process was investigated by FTIR spectroscopy. Spectra of the IgG standard in aqueous medium and in the presence of the ionic liquid [Ch]Cl were recorded at the same temperatures used in the partitioning experiments (Figure 7). The characteristic absorption bands of both IgG and the ionic liquid were clearly identified in all systems. Notably, despite temperature variations, the spectral features of IgG in the bottom phase remained stable, with no significant shifts or intensity changes.

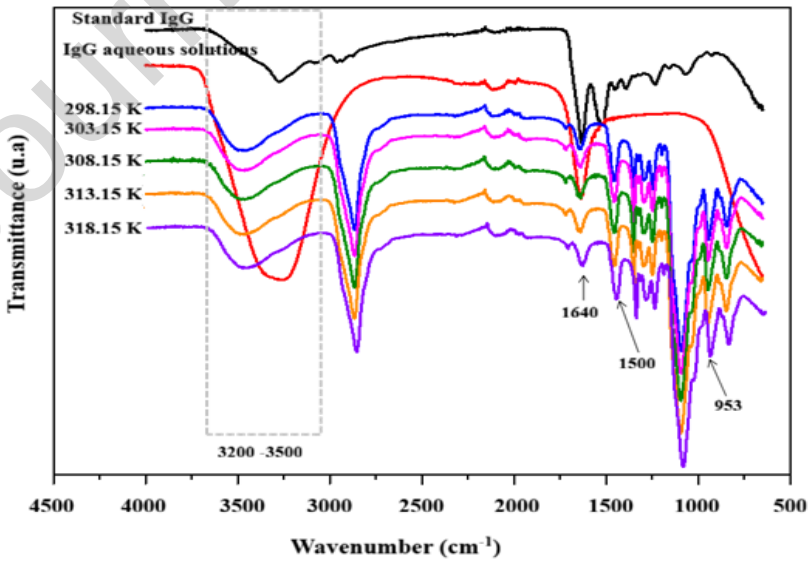

Figure 7. FTIR spectra of standard IgG (—), aqueous IgG solution (—), and bottom phases of ATPSs containing IgG and [Ch]Cl at different temperatures such as (—) 298 K, (—) 303 K, (—) 308 K, (—) 213 K; (—) 318 K.

This behavior indicates the absence of relevant conformational alterations in IgG, particularly in the amide I region (≈1650 cm^{-1}), which is highly sensitive to changes in protein secondary structure. The preservation of this band up to 318 K suggests that IgG maintains its structural integrity under the experimental conditions evaluated, confirming the suitability of the partitioning process for applications requiring protein stability.

Deconvolution of the FTIR spectra in the 1600–1700 cm^{-1} region (Figure 8) was performed to investigate the secondary structure of IgG. The results obtained for IgG in the presence of the ionic liquid [Ch]Cl at different temperatures did not reveal conformational alterations indicative of protein denaturation or precipitation. Comparative analysis revealed that the IgG standard spectrum (Figure 8A) exhibited the lowest content of β-sheet and β-turn structures, with α-helix content predominating and displaying well-defined, isolated bands.

This structural profile remained stable under the evaluated conditions, indicating that IgG did not undergo significant conformational changes that could compromise its structural integrity and, consequently, its functional properties. In contrast, the spectra shown in Figure 8E, corresponding to IgG partitioned at 318 K, revealed an increase in β-structure content along with a noticeable overlap between α-helix and β-turn bands. This behavior suggests more pronounced alterations in the protein secondary structure at higher temperatures, possibly reflecting partial conversion of α-helix structures into β-turn or β-sheet conformations.

Protein thermal denaturation is commonly described as a two-stage process: (i) reversible unfolding of the native structure, followed by (ii) irreversible aggregation and/or chemical modifications that ultimately lead to a denatured, often insoluble state [67]. A parallel can be drawn with the study by Usoltsev et al. [68], which supports the methodological approach adopted in the present work. In that study, human serum albumin (HSA) was subjected to temperatures ranging from 323 to 343 K, and conformational stability was monitored through changes in the amide I region of the spectrum. The authors reported that HSA aggregation begins at approximately 329 K, characterized by a pronounced loss of α-helix content and a concomitant increase in β-sheet structures, indicating partial protein unfolding. This process was quantified by an approximately 2.3-fold reduction in α-helix content, reflecting a significant structural rearrangement toward more disordered conformations. In contrast, the results obtained for IgG in the present study demonstrate conformational stability up to 318 K, with no analogous α-helix–to–β-sheet transition observed in the amide I region. These findings

suggest that IgG exhibits higher thermal resistance under the investigated conditions, thereby reinforcing its structural robustness during the partitioning process.

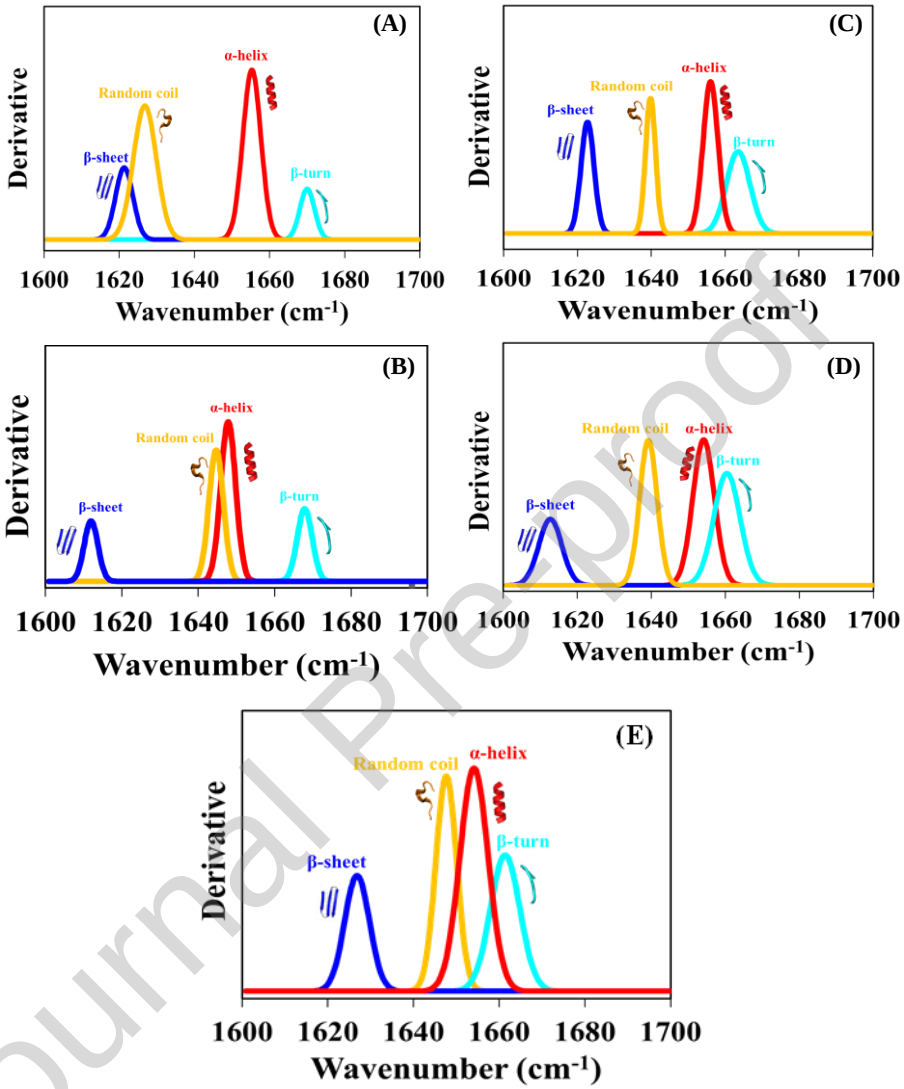

Figure 8. Deconvoluted FTIR (secondary-derivative) spectra in the amide I region (1,700–1,600 cm^{-1}) of IgG in ATPSS formed by PEGME 550 (45 wt%) + [Ch]Cl (40 wt%) + water (15 wt%) at different temperatures: (A) – 298 K; (B) – 303 K; (C) – 308 K; (D) – 313 K and (E) – 318 K.

The combined results from electrophoretic (SDS-PAGE) analysis and FTIR spectral evaluation of the amide I region confirm the structural integrity of IgG under the experimental conditions investigated. In the SDS-PAGE analysis, samples collected from both phases of the system—the PEGME 550–rich top phase and the [Ch]Cl–rich bottom phase—obtained at 298.15 K with 40 wt% [Ch]Cl, displayed the characteristic IgG bands

at the expected molecular weights of approximately 50 kDa (heavy chain) and 25 kDa (light chain), with no evidence of degradation products. This electrophoretic evidence, together with the preservation of the conformational profile observed in the amide I region by FTIR, conclusively demonstrates that no significant denaturation or degradation of IgG occurred during the partitioning process.

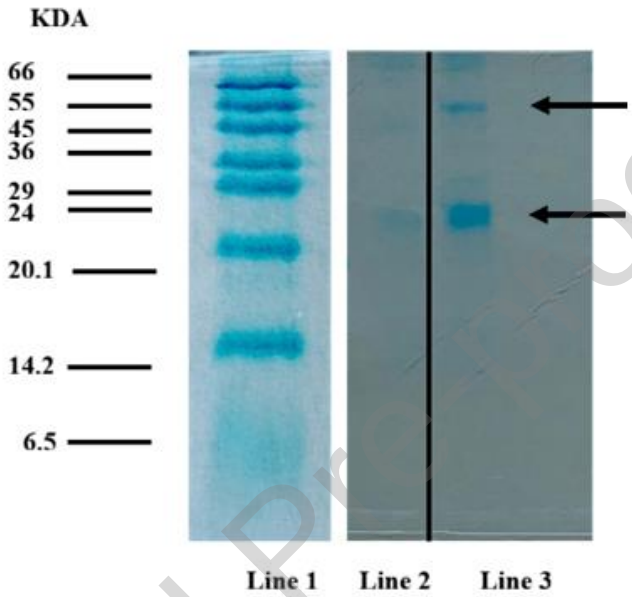

Figure 9. SDS-PAGE stained with coomassie blue (12 wt% gel) of the phases of the ATPSs formed by PEGME 550 (45 wt%) + [Ch]Cl (40 wt%) + aqueous solution of IgG (15 wt% - 1 mg mL^{-1}) system at 298.15 K and 0.1 MPa. Lanes: (1) molecular weight marker and IgG standard; (2) top phase of the system (PEGME 550–rich polymer phase); (3) bottom phase of the system ([Ch]Cl–rich phase containing IgG).

4. Conclusion

This work demonstrates that ATPSs composed of PEGME 550 and cholinium-based ionic liquids can be successfully formed and further investigated as promising platforms for separation processes. Phase formation is primarily driven by hydrogen-bonding, indicating that intermolecular interactions play a central role in phase separation.

BSA was initially employed as a model protein to evaluate partitioning behavior in systems composed of PEGME 550 (45 wt%) and cholinium-based ionic liquids (40 wt%) at 298 K and 0.1 MPa. Among the ionic liquids investigated, [Ch]Cl was identified as the most suitable for protein partitioning, as it promoted preferential migration of BSA

to the bottom phase (K_{BSA} = 0.81±0.04). However, the extraction efficiency in the bottom phase remained low ($[EE_{BSA}]_B$ = 50.31 ± 1.30 %). This system also exhibited minimal impact on protein structural stability, as confirmed by FTIR spectroscopy. The applicability of this system was extended to IgG, enabling optimization of partitioning conditions. The lowest K_{IgG} (0.70 ± 0.01) was obtained for the system composed of PEGME 550 (45 wt%) and [Ch]Cl (40 wt%) at 298 K and 0.1 MPa; however, the extraction efficiency remained relatively low ($[EE_{IgG}]_B$ = 48.68 ± 0.33 %). Partitioning trends were further supported by molecular docking simulations, which revealed specific interactions between the cholinium-based ionic liquid ions and the protein surfaces. Thermodynamic analysis indicated that IgG partitioning toward the target phase is non-spontaneous ($\Delta G > 0$), suggesting a preference for the ionic liquid-rich (bottom) phase. The process was found to be exothermic, with entropy contributions dominating the overall thermodynamic balance. FTIR spectroscopy confirmed that IgG maintained its structural integrity under optimized conditions, as further supported by SDS-PAGE analysis, which showed intact protein bands at approximately 50 kDa and 25 kDa, corresponding to the heavy and light chains, respectively.

Overall, the results here presented demonstrate that proteins retain their structural integrity in PEGME 550–[Ch]Cl ATPSs, while preferentially partitioning to the bottom IL-rich phase. However, further studies are required to infer their selectivity and potential to purify high-value proteins from complex biological media.

Acknowledgements

The authors would like thank the financial agencies *Coordenação de Aperfeiçoamento de Pessoal de Nível Superior* – CAPES, and *Conselho Nacional de Desenvolvimento Científico e Tecnológico* – CNPq (A.S. Lima - Grant number 306073/2023-4); FCT, Portugal for the support within the projects DOI: 10.54499/UIDB/00102/2020 (Base funding) and DOI: 10.54499/UIDP/00102/2020 (Programmatic funding). This work was developed within the scope of the project CICECO – Aveiro Institute of Materials, UID/50011/2025 (DOI 10.54499/UID/50011/2025) & LA/P/0006/2020 (DOI 10.54499/LA/P/0006/2020), financed by national funds through the FCT/MCTES (PIDDAC).

CRediT authorship contribution statement

Tairan Eutimio dos Santos: Methodology, Formal analysis and Writing – original draft. **Milena Santos Leite:** Methodology and Formal analysis. **Ranyere Lucena de Souza:** Formal analysis. **Matheus Mendonça Pereira:** Data curation and Software. **Mara G. Freire:** Conceptualization and Validation. **Cleide Mara Faria Soares:** Supervision. **Álvaro Silva Lima:** Supervision, Funding acquisition, Project administration and Writing – review and editing.

Declaration of competing interest

The authors declare that they have no known competing financial interests or personal relationships that could have appeared to influence the work reported in this paper.

Data availability

Data will be made available on request.

References

[1] B, Michael, M.T. Neves, R.C.S. Sousa, M.M. Chagas, B.A. Martins, J.S.R. Coimbra, Partição de proteínas de soro de leite em sistemas aquosos bifásicos baseados em líquidos iônicos, Quim. Nova. 38 (2015) 1148–1152. https://doi.org/10.5935/0100-4042.20150123

[2] H. Tian, P. Berton, R.D. Rogers, Choline-based aqueous biphasic systems: Overview of applications, Fluid Phase Equilibr. 502 (2019) 112258. https://doi.org/10.1016/j.fluid.2019.112258

[3] A.L. Grilo, M.R. Aires-Barros, A.M. Azevedo, Partitioning in aqueous two-phase systems: fundamentals, applications and trends, Sep. Purif. Rev. 45 (2016) 68–80.

[4] C.M.S.S. Neves, S. Shahriari, J. Lemus, J.F.B. Pereira, M.G. Freire, J.A.P. Coutinho, Aqueous biphasic systems composed of ionic liquids and polypropylene glycol: insights into their liquid–liquid demixing mechanisms, Phys. Chem. Chem. Phys. 18 (2016) 20571–20582. https://doi.org/10.1039/C6CP04023C

[5] Berton, H. Tian, R.D. Rogers, Phase behavior of aqueous biphasic systems with choline alkanoate ionic liquids and phosphate solutions: The influence of pH, Molecules. 26 (2021) 1702, https://doi.org/10.3390/molecules26061702

[6] A.M. Azevedo, P.A.J. Rosa, I.F. Ferreira, M.R. Aires-Barros, Optimisation of aqueous two-phase extraction of human antibodies, J. Biotechnol. 132 (2007) 209–217, https://doi.org/10.1016/j.jbiotec.2007.04.002

[7] A.F.C.S. Rufino, M.R. Almeida, M. Sharma, J.A.P. Coutinho, M.G. Freire, Separation of albumin from bovine serum applying ionic-liquid-based aqueous biphasic systems, Appl. Sci. 12 (2022), 707, https://doi.org/10.3390/app12020707

[8] M.S. Álvarez, F.J. Deive, A. Rodríguez, M.A. Longo, Designing biodegradable aqueous biphasic systems for the selective separation of enzymes, Sep. Purific. Technol 353 (2025) 128508, https://doi.org/10.1016/j.seppur.2024.128508.

[9] K. Xu, Y. Zhao, K. Chen, H, Dong, S.Sun, Z. Ni, Y. Wang. Aqueous biphasic systems developed with deep eutectic solvents and polymer for the efficient extraction of pigments from beverages, Food Chem. 449 (2024) 139206, https://doi.org/10.1016/j.foodchem.2024.139206.

[10] J.H. Santos, F.A. Silva, S.P.M. Ventura, J.A.P. Coutinho, R.L. Souza, C.M.F. Soares, A.S. Lima, Ionic liquid-based aqueous biphasic systems as a versatile tool for the recovery of antioxidant compounds, Biotechnol. Prog. 31 (2015) 70–77, https://doi.org/10.1002/btpr.2000

[11] S.K. Shukla, S. Pandey, S. Pandey, Applications of ionic liquids in biphasic separation: Aqueous biphasic systems and liquid–liquid equilibria, J. Chromatogr. A, 1559 (2018) https://doi.org/10.1016/j.chroma.2017.10.019

[12] M.B. Nascimento, S.S. Castro, C.M. Veloso, R.C.I. Fontan, D.J.S. Nascimento, O.R.R. Gandolfi, V.S. Sampaio, L.A.A. Veríssimo, R.C.F. Bonomo. Equilibrium data and thermodynamic studies of α-amylase partition in aqueous two-phase systems. Fluid Phase Equilibr. 463 (2018) 69–79, https://doi.org/10.1016/j.fluid.2018.02.005

[13] A. Santos, P.G.C. Gomes, F.S. Buarque, C.M.F. Soares, T.R. Bjerk, A.S. Lima, Novel strategy for extraction and partitioning of phenol compounds from industrial residue of seriguela (*Spondia purpurea* L.) using aqueous two-phase systems, Food Bioprod. Process. 141 (2023) 219–229, https://doi.org/10.1016/j.fbp.2023.08.011

[14] C.X. Zeng, R.P. Xin, S.J. Qi, B. Yang, Y.H. Wang, Aqueous two-phase system based on natural quaternary ammonium compounds for the extraction of proteins, J.Sep. Sci. 39 (2016) 648–654, https://doi.org/10.1002/jssc.201500660

[15] R.L.S.F. Rosário, R.L. Souza, R.L. F.O. Farias, M.R. Mafra, C.M.F. Soares, H. Passos, J.A.P. Coutinho, A.S. Lima, Acetonitrile as adjuvant to tune polyethylene glycol + K_3PO_4 aqueous two-phase systems and its effect on phenolic compounds

partition, Sep. Technol. Purif. 223 (2019) 41–48. https://doi.org/10.1016/j.seppur.2019.04.062

[16] S. Keskin, D. Kayrak-Talay, U. Akman, O, Hortaçsu, A review of ionic liquids towards supercritical fluid applications, J. Supercrit. Fluid. 43 (2007) 150–180, https://doi.org/10.1016/j.supflu.2007.05.013

[17] K.N. Marsh, J.A. Boxall, R. Lichtenthaler, Room temperature ionic liquids and their mixtures: a review, Fluid Phase Equilibr. 219 (2004) 93–98, https://doi.org/10.1016/j.fluid.2004.02.003

[18] M.A. Even, C. Chen, J. Wang, Z. Chen, Chemical structures of liquid poly(ethylene glycol)s with different end groups at buried polymer interfaces, Macromolecules. 39 (2006) 9396–9401, https://doi.org/10.1021/ma061785h

[19] J.F.B. Pereira, K.A. Kurnia, M.G. Freire, J.A.P. Coutinho, R.D. Rogers, Controlling the formation of ionic-liquid-based aqueous biphasic systems by changing the hydrogen-bonding ability of polyethylene glycol end groups, Chem. Phys. Chem. 16 (2015) 2219–2225, https://doi.org/10.1002/cphc.201500146

[20] P. Panas, C. Lopes, M.O. Cerri, S.P.M. Ventura, V.S. Santos-Ebinuma, J.F.B. Pereira. Purification of clavulanic acid produced by streptomyces clavuligerus via submerged fermentation using polyethylene glycol/cholinium chloride aqueous two-phase systems, Fluid Phase Equilibr. 450 (2017) 42–50, https://doi.org/10.1016/j.fluid.2017.07.005

[21] P.L. Santos, L.N.S. Santos, S.P.M. Ventura, R.L. Souza, J.A.P. Coutinho, C.m.F. Soares, A.S. Lima. Recovery of capsaicin from *Capsicum frutescens* by applying aqueous two-phase systems based on acetonitrile and cholinium-based ionic liquids, Chem. Eng. Res. Des. 112 (2016) 103–112, https://doi.org/10.1016/j.cherd.2016.02.031

[22] C.C. Ramalho, C.M.S.S. Neves, M.V. Quental, J.A.P. Coutinho, M.G. Freire, Separation of immunoglobulin G using aqueous biphasic systems composed of cholinium-based ionic liquids and poly(propylene glycol), J. Chem. Technol. Biotechnol. 93 (2018) 1931–1939, https://doi.org/10.1002/jctb.5594

[23] A.M.S. Jorge, J.F.B. Pereira, Aqueous two-phase systems – versatile and advanced (bio)process engineering tools, Chem. Commun. 60 (2024) 12144–12168, https://doi.org/10.1039/D4CC02663B

[24] Y. Bai, S. Sun, H. Zhang, T. Zhao, Investigation of interaction between bovine serum albumin and drugs by fluorescence spectrometry. Anal. Methods. 5 (2013) 7036–7041, https://.org/10.1039/C3AY41008K

[25] C. Guo, X. Guo, W. Chu, N. Jiang, H. Li, Spectroscopic study of conformation changes of bovine serum albumin in aqueous environment, Chin. Chem. Lett. 30 (2019) 1302–1306, https://doi.org/10.1016/j.cclet.2019.02.023

[26] N.S. Greenspan, L.A. Cavacini, Immunoglobulin function, in: Clinical immunology: Principles and practice, Elsevier, Amsterdam, 2019, pp. 223–233

[27] Z. Wang, G. Wang, H. Lu, H. Li, M. Tang, A. Tong, Development of therapeutic antibodies for the treatment of diseases, Mol. Med. 3 (2022) 35, https://doi.org/10.1186/s43556-022-00100-4

[28] M. Taha, M.R. Almeida, F.A. Silva, P. Domingues, S.P.M. Ventura, J.A.P. Coutinho, M.G. Freire, Novel biocompatible and self-buffering ionic liquids for biopharmaceutical applications, Chem. Eur. J. 21 (2015) 4781–4788, https://doi.org/10.1002/chem.201405693

[29] F.S. Buarque, D.E.M. Guimarães, C.M.F. Soares, R.L. Souza, M.M. Pereira, A.S. Lima, Ethanolic two-phase system formed by polypropylene glycol, ethylene glycol and/or ionic liquid (phase-forming or adjuvant) as a platform to phase separation and partitioning study, J. Mol. Liq. 344 (2021) 117702, https://doi.org/10.1016/j.molliq.2021.117702

[30] T.S.P. Lima, M.M. Borges, F.S. Buarquem R.L. Souza, C.M.F. Soares, A.S. Lima. Purification of vitamins from tomatoes (*Solanum lycopersicum*) using ethanolic two-phases systems based on ionic liquids and polypropylene glycol, Fluid Phase Equilibr. 557 (2022) 113434, https://doi.org/10.1016/j.fluid.2022.113434

[31] J.C. Merchuk, B.A. Andrews, J.A. Asenjo. Aqueous two-phase systems for protein separation: Studies on phase inversion, J. Chromatogr. B Biomed. Appl. 711 (1998) 285–293, https://doi.org/10.1016/S0378-4347(97)00594-X

[32] M.M. Bradford, A rapid and sensitive method for the quantitation of microgram quantities of protein utilizing the principle of protein-dye binding, Anal. Biochem. 72 (1976) 1–2, https://doi.org/10.1016/0003-2697(76)90527-3

[33] O. Trott, A.J, Olson. AutoDock Vina: Improving the speed and accuracy of docking with a new scoring function, efficient optimization, and multithreading, J. Comput. Chem. 31 (2010) 455–461, https://doi.org/10.1002/jcc.21334

[34] G.M. Morris, R. Huey, W. Linstrom, M.F. Sanner, R.K. Belew, D.S. Goodsell, A.J. Olson. AutoDock4 and AutoDockTools4: Automated docking with selective receptor flexibility, J. Comput. Chem. 30 (2009) 2785–2791, https://doi.org/10.1002/jcc.21256

[35] U.K. Laemmli, Cleavage of structural proteins during assembly of head of bacteriophage-T4, Nature, 227 (1970) 680–685, https://doi.org/10.1038/227680a0

[36] M.T. Zafarani-Moattar, H. Shekaari, P. Jafari, Structural effects of choline amino acid ionic liquids on the extraction of bovine serum albumin by green and biocompatible aqueous biphasic systems composed of polypropylene glycol400 and choline amino acid ionic liquids, J. Mol. Liq. 301 (2020) 112397, https://doi.org/10.1016/j.molliq.2019.112397

[37] P. Bharmoria, A. Kumar, Thermodynamic investigations of protein's behaviour with ionic liquids in aqueous medium studied by isothermal titration calorimetry, Biochim. Biophys. Acta. 1860 (2016) 1017–1025, https://doi.org/10.1016/j.bbagen.2015.08.022

[38] M.V. Lomova, A.I. Brichkina, M.V. Kiryukhin, E.N. Vasina, A.M. Pavlov, D.A. Gorin, G.B. Sukhorukov, M.N. Antipina, Multilayer capsules of bovine serum albumin and tannic acid for controlled release by enzymatic degradation, ACS Appl. Mater. Interfaces. 7 (2015), 11732–11740, https://doi.org/10.1021/acsami.5b03263

[39] C.P. Song, R.N. Ramanan, R. Vijayaraghavan, D.R. MacFarlane, E.S. Chan, C.W. Ooi, Green, aqueous two-phase systems based on cholinium aminoate ionic liquids with tunable hydrophobicity and charge density, ACS Sustain. Chem. Eng. 3 (2015) 3291–3298, https://doi.org/10.1021/acssuschemeng.5b00881

[40] Z. Du, Y,L. Yu, J.H. Wang, Extraction of proteins from biological fluids by use of an ionic liquid/aqueous two-phase system, Chem. Eur. J. 13 (2007) 2130–2137, https://doi.org/10.1002/chem.200601234

[41] S. Dreyer, P. Salim, U. Kragl, Driving forces of protein partitioning in an ionic liquid-based aqueous two-phase system, Biochem. Eng. J. 46 (2009) 176–185, https://doi.org/10.1016/j.bej.2009.05.005

[42] M.V. Quental, M. Caban, M.M. Pereira, P. Stepnowski, J.A.P. Coutinho, M.G. Freire, Enhanced extraction of proteins using cholinium-based ionic liquids as phase-forming components of aqueous biphasic systems, Biotechnol. J. 10 (2015) 1457–1466, https://doi.org/10.1002/biot.201500003)

[43] M.T. Zafarani-Moattar, H. Shekaari, P. Jafari, Thermodynamic study of aqueous two-phase systems containing biocompatible cholinium aminoate ionic-liquids and polyethylene glycol di-methyl ether 250 and their performances for bovine serum albumin separation, J. Chem. Thermodyn. 130 (2019) 17–32, https://doi.org/10.1016/j.jct.2018.10.001

[44] S. Huang, Y. Wang, Y. Zhou, L. Li, Q. Zeng, X. Ding, Choline-like ionic liquid-based aqueous two-phase extraction of selected proteins, Analytical Methods. 5 (2013) 3395–3402, https://doi.org/10.1039/C3AY40377G

[45] M.T. Zafarani-Moattar, H. Shekaari, P. Jafari, Thermodynamics of acetaminophen and bovine serum albumin partitioning in ternary aqueous solutions comprising polyethylene glycol dimethyl ether 250 and choline bitartrate: Liquid-liquid equilibria, volumetric and acoustic investigations, J. Mol. Liq. 323 (2021) 115072, https://doi.org/10.1016/j.molliq.2020.115072

[46] M.T. Zafarani-Moattar, H. Shekaari, P. Jafari, Design of novel biocompatible and green aqueous two-phase systems containing cholinium l-alaninate ionic liquid and polyethylene glycol di-methyl ether 250 or polypropylene glycol 400 for separation of bovine serum albumin (BSA), J. Mol. Liq. 254 (2018) 322–332, https://doi.org/10.1016/j.molliq.2018.01.094

[47] A.B.D. Nandiyanto, R. Oktiani, R. Ragadhita, How to read and interpret FTIR spectroscope of organic material. Indones. J. Sci. Technol. 4 (2019) 97–118, 10.17509/ijost.v4i1.15806

[48] M.S. Barbosa, C.C.C. Freire, L.M.S. Brandão, E.B. Pereira, A.A. Mendes, M.M. Pereira, A.S. Lima, C.M.F. Soares, Biolubricant production under zero-waste Moringa oleifera Lam biorefinery approach for boosting circular economy, Ind. Crop. Prod. 167 (2021) 113542, https://doi.org/10.1016/j.indcrop.2021.113542

[49] D. Yue, Y.Z. Jia, Y. Yao, J. Sun, Y Jing. Structure and electrochemical behavior of ionic liquid analogue based on choline chloride and urea, Electrochim. Acta. 65 (2012) 30–36, https://doi.org/10.1016/j.electacta.2012.01.003

[50] D. Mondal, M. Sharma, M.V. Quental, A.P.M. Tavares, K. Prasad, M.G. Freire. Suitability of bio-based ionic liquids for the extraction and purification of IgG antibodies, Green Chem. 18 (2016) 6071–6081, https://doi.org/10.1039/C6GC01482H

[51] T.A. Shmool, L.K. Martin, R.P. Matthews. J.P. Hallett, Ionic liquid-based strategy for predicting protein aggregation propensity and thermodynamic stability, JACS Au. 2 (2022) 2068–2080, https://doi.org/10.1021/jacsau.2c00356

[52] A. Barth, Infrared spectroscopy of proteins, Biochim. Biophys. Acta - Bioenerg. 1767 (2007) 1073–1101, https://doi.org/10.1016/j.bbabio.2007.06.004

[53] P. Bourassa, C.D. Kanakis, P. Tarantilis, M.G. Pollissiou, H.A. Tajmir-Riahi, Resveratrol, genistein, and curcumin bind bovine serum albumin, J. Phys. Chem. B. 114 (2010) 3348–3354, https://doi.org/10.1021/jp9115996

[54] L. Cheng, H. Huang, J Zeng, Z. L., X. Tong, Z. Li, H. Zhao, F. Dai, Effect of different additives in diets on secondary structure, thermal and mechanical properties of silkworm silk, Materials. 12 (2019) 14, https://doi.org/10.3390/ma12010014

[55] D. Spelzini, G. Darío, B. Farruggia, Dependence of chymosin and pepsin partition coefficient with phase volume and polymer pausidispersity in polyethyleneglycol–phosphate aqueous two-phase system, Colloids Surf B Biointerfaces. 51 (2006) 80–85, https://doi.org/10.1016/j.colsurfb.2006.03.023

[56] Y.H. Chow, Y.J. Yap, P.L. Show, J.C. Juan, M.S. Anuar, E.P. Ng, C.W. Ooi, T.C. Ling, Characterization of partitioning behaviors of immunoglobulin G in polymer-salt aqueous two-phase systems, J. Biosci. Bioeng. 122 (2016) 613–619, https://doi.org/10.1016/j.jbiosc.2016.04.008

[57] J.M.P. Barbosa, R.L, Souza, A.T. Fricks, G.M. Zanin, C.M.F. Soares, A.S. Lima, Purification of lipase produced by a new source of *Bacillus* in submerged fermentation using an aqueous two-phase system, J. Chromatogr. B. 879 (2011) 3853–3858, https://doi.org/10.1016/j.jchromb.2011.10.035

[58] C. He, S. Li, H. Liu, K. Li, F. liu, Extraction of testosterone and epitestosterone in human urine using aqueous two-phase systems of ionic liquid and salt, J. Chromatogr. A. 1082 (2005) 143–149, https://doi.org/10.1016/j.chroma.2005.05.065

[59] Y. Pei, J. Wang, K. Wu, X. Xuan, X. Lu, Ionic liquid-based aqueous two-phase extraction of selected proteins, Sep. Purif. Technol. 64 (2009) 288–295, https://doi.org/10.1016/j.seppur.2008.10.010

[60] H.A. Mahdi, K.W. Hameed, A.J.A. Ali, Extraction of bovine serum albumin by aqueous two-phase system using PEG4000/sodium citrate and PEG8000/sodium phosphate, Khwarizmi Eng. J. 19 (2023) 39–51, https://doi.org/10.22153/kej.2023.04.001

[61] Y. Pei, L. Li, Z. Li, C. Wu. J. Wang, Partitioning behavior of wastewater proteins in some ionic liquids-based aqueous two-phase systems, Sep. Sci. Technol. 47 (2012) 277–283, https://doi.org/10.1080/01496395.2011.609241

[62] V.S. Sampaio, R.C.F. Bonomo, C.M. Veloo, R.C.S. Sousa, E.C.S. Júnior, R.C.I. Fontan, M.C. Pignata, K.A. Santos, O.R.R. Gandolfi. Partitioning behavior of lysozyme and α-lactalbumin in aqueous two-phase system formed by ionic liquids and potassium phosphate, Int. J. Food Eng. 13 (2017) 20170274, https://doi.org/10.1515/ijfe-2017-0274

[63] D. Bogahawaththa, J. Chandrapala, T. Vasiljevic, Thermal denaturation of bovine immunoglobulin G and its association with other whey proteins, Food Hydrocoll. 72 (2017) 350–357, https://doi.org/10.1016/j.foodhyd.2017.06.017

[64] B. Perez, L.P. Malpiedi, G. Túbio, B. Nerlo, P.A. Pêssoa Filho, Experimental determination and thermodynamic modeling of phase equilibrium and protein partitioning in aqueous two-phase systems containing biodegradable salts, J. Chem. Thermodyn. 56 (2013) 136-143, https://doi.org/10.1016/j.jct.2012.07.017

[65] P.A. Pêssoa Filho, R.S. Mohamed, Thermodynamic modelling of the partitioning of biomolecules in aqueous two-phase systems using a modified Flory-Huggins equation, Process Biochem. 39 (2004) 2075-2083, https://doi.org/10.1016/j.procbio.2003.10.012

[66] D. Dhiman, M. Bisht, A.P.M. Tavares, M.G. Freire, P. Venkatesu. Cholinium-based ionic liquids as efficient media for improving the structural and thermal stability of immunoglobulin G antibodies, ACS Sustain. Chem. Eng. 10 (2022) 5404–5420, https://doi.org/10.1021/acssuschemeng.1c07979

[67] S. Era, K.B. Itoh, M. Sogami, K.Kuwata, T. Iwama, H. Yamada, H.W. Atari, Structural transition of bovine plasma albumin in the alkaline region the N-B transition, Int. J. Pept. Protein. Res. 35 (1990) 1–11, https://doi.org/10.1111/j.1399-3011.1990.tb00714.x

[68] D. Usoltsev, V. Sitnikova, A. Kajava, M. Uspenskaya. Systematic FTIR spectroscopy study of the secondary structure changes in human serum albumin under various denaturation conditions. Biomolecules, 9 (2019) 359, https://doi.org/10.3390/biom9080359

Declaration of interests

☒ The authors declare that they have no known competing financial interests or personal relationships that could have appeared to influence the work reported in this paper.

☐ The authors declare the following financial interests/personal relationships which may be considered as potential competing interests:

Graphical abstract

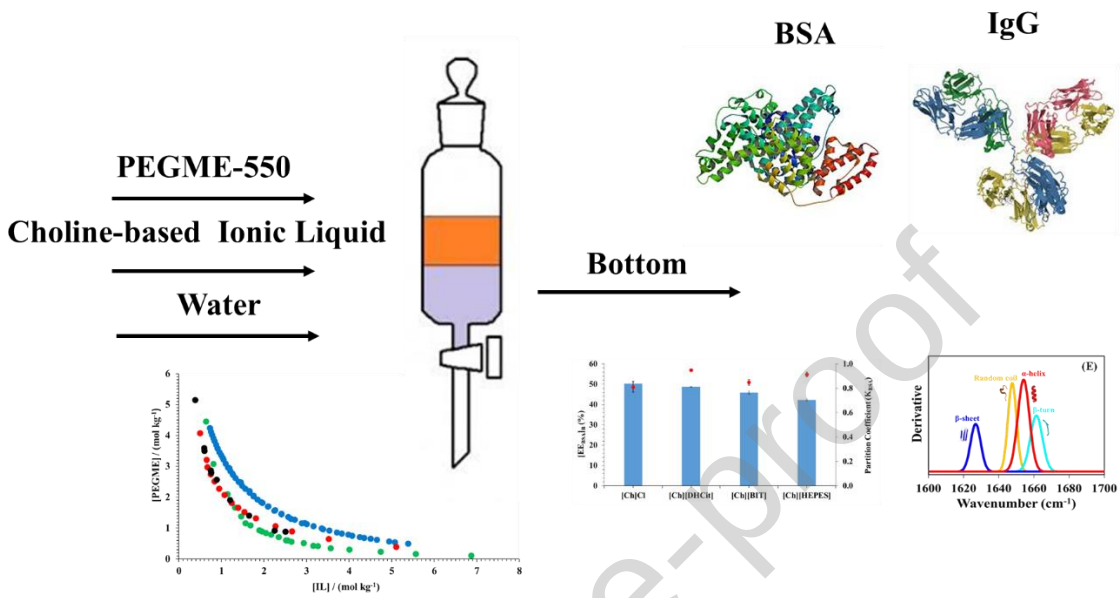

Highlights

- ATPS composed of PEGME 550 and cholinium-based ionic liquids can be formed
- Phase formation is primarily driven by intermolecular interactions
- Optimal BSA (K=0.81) and IgG (K=0.70) partitioning was achieved in [Ch]Cl-based ATPS
- Molecular docking simulations confirmed the experimental partitioning trends
- FTIR spectroscopy confirmed the structural integrity of IgG after separation